2022

Modified Exergy Analysis of a Two-stage Refrigeration System for a Battery Electric Vehicle

George Luiz Rincaweski Vegini

Guilherme Ribeiro

Modified Exergy Analysis of a Two-stage Refrigeration System for a Battery Electric Vehicle

George Luiz Rincaweski VEGINI[1*], Guilherme Borges RIBEIRO[1]

[1] Aeronautics Institute of Technology, Department of Mechanical Engineering,
São José dos Campos, São Paulo, Brazil
georgev@ita.br
gbribeiro@ita.br

* Corresponding Author

ABSTRACT

As a manner to decrease greenhouse emission, the used hybrid powertrain and battery electric vehicles (BEV) has increased considerably in the last years. Thus, an efficient thermal management system of BEV must take into account the battery heat removal and the mobile air-conditioning, making a direct cooling scheme that consists of two-stage refrigeration where one evaporator is addressed to the vehicle cabin, whereas the other is addressed to the battery pack. Focusing on these refrigeration systems, steady-state endoreversible modeling is proposed. The heat dissipated by the battery pack and the indoor and outdoor air conditions are applied as input conditions. Global thermal conductances are considered for all heat exchangers, considering different fluid phases. A scroll compressor with fixed volumetric and global efficiencies is modeled. The thermodynamic states throughout the cycle are achieved numerically by the means of successive substitutions. To evaluate the system performance, the modified exergy analysis (MEA) is implemented in this study. Employing this analysis, the amount of exergy destruction is split between the refrigerant and any system component. Furthermore, the refrigerant fluids R-1234ze, R-1234yf, and R-32 are applied and compared to the baseline fluid R-134a. This proper evaluation of the source of the exergy destruction will serve as a guide to enhance the performance of vapor compression systems commonly used BEV thermal management.

1. INTRODUCTION

Human induced climate change is a serious threat for human life on earth, mainly due to anthropogenic related greenhouse gases emission since the beginning of the industrialization process (Howe, 2015). Transportation is a significant source of greenhouse gases emissions, thus, there has been a transition in the automotive market from internal combustion to electric vehicles (EV) (IEA, 2019).

Battery electric vehicle is the most common type of EV, being the Li-ion battery the most used. Li-ion battery is very sensitive to temperature for its functioning, as operating outside its ideal ranges can cause thermal runaway and reduces drastically the battery power and life cycle (Wang et al., 2016). Therefore, an efficient and compact scheme of battery thermal management system is a crucial aspect that must be taken into account when designing an EV. Technologies for battery thermal management are: air cooling, liquid cooling, direct refrigerant cooling, phase change material, heat pipe cooling, and thermoelectric cooling (Kim et al., 2019). Focusing on direct refrigerant cooling, a vapor-compression refrigeration system (VCRS) can be used to extract the battery heat and provide cabin temperature comfort through two distinct evaporators connected to the same compressor, such structure is called a two-stage refrigeration system.

Although vapor-compression multi-pressure system is a technology already used in industrial refrigeration (Stoecker & Jones, 1983) and at vehicles for specific purposes (Peuker & Hrnjak, 2006), it is not a common practice at EVs. Kim et al. (2019) even mentions that there are few studies on the theme. Exceptions are Krüger et al. (2012), Gillet et al. (2016) and Shelly et al. (2021).

There is yet another issue to be considered, most of the refrigerant fluids used in the current automotive vapor-compression refrigeration system are hydrofluorocarbons, some of which also have a high potential for global warming (GWP). R-134a, which is the most used has high GWP. There are, however, alternatives to be considered. R-32, has medium GWP, and other fourth generation refrigerants, like R-1234yf and R-1334ze(e), have negligible GWP (Myhre et al., 2013).

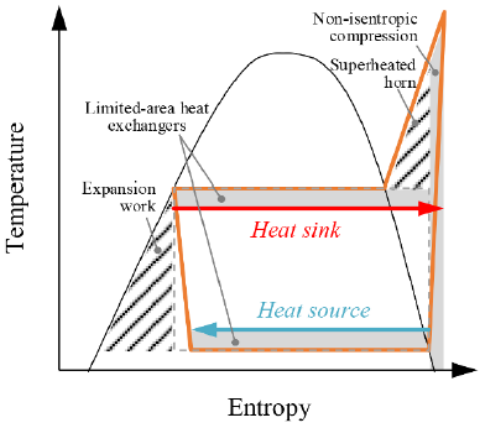

Figure 1: Sources of refrigerant exergy destruction (Cui et al., 2022).

Entropy generation or conventional exergy analysis (CEA), based on the second law of thermodynamics, is a classic method for depicting the irreversible loss distribution in VCRS. Although a powerful tool of analysis, the CEA is not capable of identifying if the loss is caused by the component itself or if it is associated with the refrigerant (Cui et al., 2022). Cui et al. (2022) developed a so called modified exergy analysis which is capable of such identification.

Firstly lets point out the sources of exergy destruction in a VCRS. The component sources of exergy destruction are directly related to those of entropy generation, that is, non-isentropic process, apparent temperature difference due to the limited heat exchanger area, and the pressure drop because of the flow resistance. Meanwhile, refrigerant sources of exergy destruction come from the fluid thermodynamic characteristics, throttling process and superheated horn (Cui et al., 2022), as shown in Figure 1.

For the MEA to split the exergy destruction of an evaluated cycle, henceforth called real cycle, into component and refrigerant portions it is firstly constructed an imaginary cycle, henceforth called ideal cycle, where all components are perfect, hence, any exergy destruction calculated comes solely from refrigerant effects. To calculate such ideal cycle the heat exchanger devices must have infinite heat exchange areas, which then leads to no difference of temperature between the device and its heat sink. The compressor must have an isentropic process (Cui et al., 2022). No other item that causes exergy destrucion by the devices must be included, such as subheating and superheating of the heat exchangers, and heat exchange from the compressor. The exergy destruction associated to a component is then the difference between the exergy destruction calculated from the real cycle and the ideal one,

$$\dot{\Psi}_d = \dot{\Psi}_{d,real} - \dot{\Psi}_{d,ideal}. \tag{1}$$

From such analysis it is also possible to calculate the exergetic efficiency of the cycle. Also called second law efficiency, η_{II}, is the ratio between the exergy recovered and the exergy supplied (Bahman & Groll, 2020), or simply, the ratio between the *COP* of the real cycle and the *COP* of the ideal one.

2. METHODOLOGY

It is considered a system that needs to refrigerate the vehicle's passenger cabin and its battery, hence, it is opted for a direct refrigerant two-phase cooling BTMS, that is, a two-stage vapor compression refrigeration cycle. The system can operate with evaporators at the same pressure or not, both configurations will be evaluated. A representation of the system is presented in Figure 2. The system with evaporators at different pressures can better cope with demand conflict from the cabin and the evaporator, but needs four expansion valves. Meanwhile, the system with evaporators at the equal pressure has the advantage of needing only one expansion valve.

To mathematically evaluate the system it is opted for an endoreversible thermodynamic model. Battery and cabin heat generations are considered as data inputs for the model. It is simplified that the system is at steady state, the devices do not lose pressure, the pipes do not exchange heat with the environment, and there is no lubricating oil.

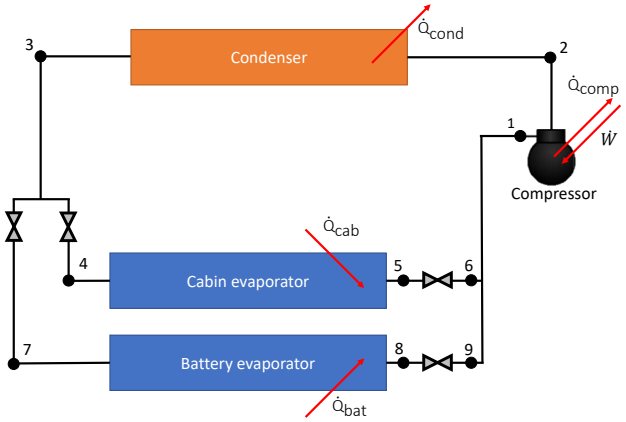

Figure 2: System considered.

2.1 Compressor

A positive displacement compressor with fixed volumetric and global efficiencies is modeled as presented by equations:

$$\eta_V = \frac{\dot{m} v_1}{Vrot}, \tag{2}$$

$$\eta_G = \frac{\dot{m}(h_{2s} - h_1)}{\dot{W}}. \tag{3}$$

From the first law of thermodynamics,

$$\dot{Q}_{comp} + \dot{W} = \dot{m}(h_2 - h_1), \tag{4}$$

and from heat transfer theory,

$$\dot{Q}_{comp} = UA_{comp}(T_{out} - T_2). \tag{5}$$

where it is considered that the compressor at the discharge temperature, T_2. Entropy generated is calculated from the second law of thermodynamics:

$$\dot{S}_{gen,comp} = \dot{m}(s_2 - s_1) - \frac{\dot{Q}_{comp}}{T_{out}}. \tag{6}$$

The amount of exergy destroyed in a process, $\dot{\Psi}_d$, which is also called irreversibility is calculated using the Gouy-Stodola theorem (Bahman & Groll, 2020):

$$\dot{\Psi}_d = T_0 \dot{S}_{gen}. \tag{7}$$

For adequate comparison between the refrigerants the authors choose to set the compressor volume for R-134a as an input and update the value for the other fluids using the relation

$$V = V_{R134a} \frac{VRE_{R134a}}{VRE}, \tag{8}$$

where *VRE* is the volumic refrigerant effect evaluated at 15°C.

2.2 Condenser

The condenser is ruled by the difference of temperature

$$\Delta T_{cond} = T_{cond} - T_{out}, \tag{9}$$

where the environment is considered a heat sink. To ensure that only liquid enters the expansion valves, temperature at state 3 is

$$T_3 = T_{cond} - \Delta T_{sub}, \tag{10}$$

The heat exchangers are discretized in zones related to the fluid phase. From the first law:

$$\dot{Q}_{cond,sh} = \dot{m}(h_{cond,v} - h_2), \tag{11}$$

$$\dot{Q}_{cond,tp} = \dot{m}(h_{cond,l} - h_{cond,v}), \tag{12}$$

$$\dot{Q}_{cond,sub} = \dot{m}(h_3 - h_{cond,l}), \tag{13}$$

and from heat transfer theory:

$$\dot{Q}_{cond,sh} = -\dot{m}c_{p,cond}\Delta T_{cond}\left[1 - \mathbf{exp}\left(-\frac{UA_{cond,sh}}{\dot{m}c_{p,cond}}\right)\right], \tag{14}$$

$$\dot{Q}_{cond,tp} = -UA_{cond,tp}\Delta T_{cond}, \tag{15}$$

$$\dot{Q}_{cond,sub} = -\dot{m}c_{p,3}\Delta T_{cond}\left[1 - \mathbf{exp}\left(-\frac{UA_{cond,sub}}{\dot{m}c_{p,3}}\right)\right]. \tag{16}$$

The entropy generated by the condenser as calculated by the second law is

$$\dot{S}_{gen,cond} = \dot{m}(s_3 - s_2) - \frac{\dot{Q}_{cond}}{T_{out}}. \tag{17}$$

2.3 Expansion Valves

The process that occurs at the expansion valves is considered isenthalpic, but not isentropic. The entropy generated at each expansion valve is

$$\dot{S}_{gen,exv} = \dot{m}(s_{out} - s_{in}). \tag{18}$$

2.4 Battery Evaporator

The battery evaporator is ruled by the difference of temperature

$$\Delta T_{bat} = T_{battery} - T_{bat}, \tag{19}$$

where the the battery is considered a heat sink. To ensure that only vapor enter the compressor:

$$T_8 = T_{bat} + \Delta T_{sup}. \tag{20}$$

Analogous to the condenser, from the first law and heat transfer theory:

$$\dot{Q}_{bat,tp} = \dot{m}_{bat}(h_{bat,v} - h_4), \tag{21}$$

$$\dot{Q}_{bat,sh} = \dot{m}_{bat}(h_5 - h_{bat,v}), \tag{22}$$

$$\dot{Q}_{bat,tp} = UA_{bat,tp}\Delta T_{bat}, \tag{23}$$

$$\dot{Q}_{bat,sh} = \dot{m}_{bat}c_{p,bat}\Delta T_{bat}\left[1 - \mathbf{exp}\left(-\frac{UA_{bat,sh}}{\dot{m}_{bat}c_{p,bat}}\right)\right]. \tag{24}$$

The amount of entropy generated as calculated by the second law is

$$\dot{S}_{gen,bat} = \dot{m}_{bat}(s_8 - s_7) - \frac{\dot{Q}_{bat}}{T_{bat}}. \tag{25}$$

2.5 Cabin Evaporator

The cabin evaporator is ruled by the difference of temperature

$$\Delta T_{cab} = T_{in} - T_{cab}, \tag{26}$$

where the cabin temperature is considered a heat sink. To ensure that only vapor enter the compressor:

$$T_5 = T_{cab} + \Delta T_{sup}. \tag{27}$$

All the other equations for cabin evaporator are equal to those of the battery evaporator adjusted for the proper states.

For closure the model of the cycle needs two more equations:

$$\dot{m} = \dot{m}_{cab} + \dot{m}_{bat}, \tag{28}$$

$$\dot{m}h_{10} = \dot{m}_{cab}h_6 + \dot{m}_{bat}h_9. \tag{29}$$

At last, the coefficient of performance of the cycle is the ratio between the sum of the heat fluxes from the evaporators and the compressor power consuption.

2.6 Numerical Approach

The system of non-linear equations are solved using an algorithm developed in python by the authors using the Coolprop package (Bell, Wronski, Quoilin, & Lemort, 2014). The algorithm uses the successive substitution method to solve the system. The results from the algorithm were validated with simulations done in the software EES (Klein, 2016).

2.7 Setting

Table 1 presents the input values to solve the model. The value where chosen by the authors based on similar systems and previous knowledge.

3. RESULTS AND DISCUSSION

To solve the mathematical model it still is needed three more inputs that will be ΔT_{cond}, ΔT_{cab} and ΔT_{bat}.

3.1 Evaporators at different pressures

Firstly, the model was solved so that ΔT_{cond},ΔT_{cab} and ΔT_{bat} were 10°C, 10°C and 20°C, respectively. Table 2 presents the results data for such system.

One can perceive that R-32 deviates the most from the others. R-32 has the worst performance of all refrigerants, specially because its operation pressure, which is greatly higher than that of the others. The product *UA* for the battery

Table 1: Input parameters

Parameter	Value	Dimension	Parameter	Value	Dimension
V_{R134a}	27.10^{-6}	m^3	p_{atm}	1.0	atm
η_G	0.6	-	ΔT_{sup}	5.0	°C
η_V	0.7	-	ΔT_{sub}	5.0	°C
T_{in}	27.0	°C	UA_{comp}	0.5	W/K
T_{out}	35.0	°C	$\dot{Q}_{cab}$	5.0	kW
$T_{battery}$	30.0	°C	$\dot{Q}_{bat}$	2.0	kW

Table 2: Results for the system with evaporators at different pressures.

	R-134a	R-1234yf	R-1234ze	R-32	Unit
COP	4.18	4.07	4.21	3.93	-
$\dot{S}_{gen}$	4.90	5.04	4.86	5.24	W/K
$\dot{m}$	0.0450	0.0570	0.0486	0.0282	kg/s
rot	122.88	126.7	123.8	118.1	Hz
$\dot{W}$	1.68	1.72	1.66	1.78	kW
p_{cond}	11.60	11.54	8.76	27.95	bar
p_{cab}	5.21	5.42	3.88	13.56	bar
p_{bat}	4.15	4.38	3.08	11.07	bar
UA_{cond}	815.5	845.4	835.1	727.6	W/K
UA_{cab}	505.9	507.8	506.3	505.1	W/K
UA_{bat}	100.5	100.6	100.5	100.4	W/K

is very inferior when compared to the condenser and the cabin. That is natural, as for the input values the heat generated by the battery is inferior to the the heat transfer in the cabin and condenser.

Figure 3 presents the percentage of entropy generated by each device for the system with evaporators at different pressures. Compressor generates the most entropy, followed by the condenser. Refrigerant R-32 deviates the most from the others having the condenser generating circa of 5% more entropy than in the others fluids. The expansion valves are the third biggest source of entropy. This is one big disadvantage from the system with evaporators at different pressures, as at any moment, there are three expansion valves at operation, causing relevant loses to the system.

Now, for the MEA it is calculated the amount of exergy destroyed in the real and ideal cycles, as presented in Table 3. Both cycles are depicted in Figure 4. Naturally, the amount of exergy destroyed by the devices for the real cycle follow the results of the percentage of entropy generated, as shown in Figure 3, having the compressor destroying the

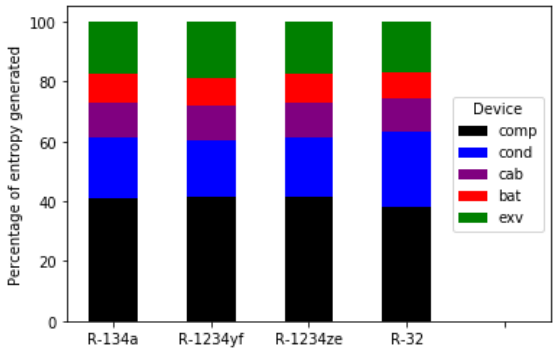

Figure 3: Percentage of entropy generated by each device for the system with evaporators at different pressures.

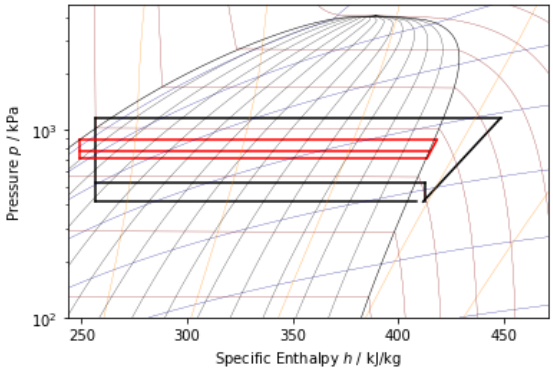

Figure 4: Pressure vs. enthalpy cycle for the system with evaporators at different pressures for R-134a. Black for real cycle and red for ideal cycle.

most exergy, followed by the condenser and expansion valves.

In the ideal cycle, the compressor destroys no exergy, as η_s = 1.0 and η_V = 1.0. The heat exchangers devices have ΔT_{cond},ΔT_{cab} and ΔT_{bat} equal to zero, as they have infinite UA. The evaporators have no superheated horn, thus they destroy no exergy. The condenser superheated horn is very small, hence its exergy destruction is minimal. The only device that presents significant exergy destruction associated purely with the refrigerant is the expansion valves, representing, 12.8%, 12.5%, 12.5%, and 14.2%, of the total exergy destroyed by those devices for R-134a, R-1234yf, R-1234ze and R-32, respectively. From these information one can perceive that the amount of exergy destruction caused by the refrigerant is almost negligible compared to the amount associated with the device.

The COP_{ideal} for R-134a, R-1234yf, R-1234ze and R-32 is 35.01, 34.43, 35.18, and 33.82, respectively, which then results to η_{II} of 0.12 for every refrigerant. The second law efficiency for all refrigerants is the same because the amount of exergy associated with the refrigerant is small, which makes the efficiency alien to the refrigerant choice. The real cycle is far from an efficient operation, mainly due to losses caused by the devices, mostly from the compressor. Thus, to improve the system a better compressor would present far better results than a change of refrigerant.

3.2 Evaporators at equal pressure

Table 4 presents the model results for inputs ΔT_{cond} = 10°C, ΔT_{cab} = 10°C, and T_{cab} = T_{bat}. Comparing with the data for the system with evaporators at different pressure (Table 2) one can perceive that this configuration has better performance. Mainly caused by the smaller power demanded by the compressor, which then reflects in smaller compressor rotation and entropy generation.

Figure 5 presents the percentage of entropy generated by each device. As the system needs less expansion valves to function, there is a significant reduction in entropy generation by such device. Therefore, in relative numbers all other devices have an increase in percentage of entropy generation, but that does not mean that there is an increase in absolute value of entropy generation, rather the contrary, there is a reduction.

Figure 6 presents the pressure vs. enthalpy cycles of both ideal and real cycles. Table 5 presents the amount of exergy destruction as calculated by the MEA. When compared to the system with evaporators at different pressures exergy

Table 3: Exergy destroyed by each component for the real and ideal cycles. Dimension for all values is W.

Device	R-134a		R-1234yf		R-1234ze		R-32	
	$\dot{\Psi}_{d,real}$	$\dot{\Psi}_{d,ideal}$	$\dot{\Psi}_{d,real}$	$\dot{\Psi}_{d,ideal}$	$\dot{\Psi}_{d,real}$	$\dot{\Psi}_{d,ideal}$	$\dot{\Psi}_{d,real}$	$\dot{\Psi}_{d,ideal}$
Compressor	616.4	0.00	646.1	0.00	621.21	0.00	616.1	0.00
Condenser	311.9	0.11	293.5	0.01	296.3	0.01	406.9	2.07
Battery evaporator	143.0	0.00	142.8	0.00	143.0	0.00	143.1	0.00
Cabin evaporator	175.5	0.00	175.1	0.00	175.5	0.00	175.7	0.00
Expansion valves	261.8	33.52	295.0	36.97	261.6	32.66	271.5	38.65

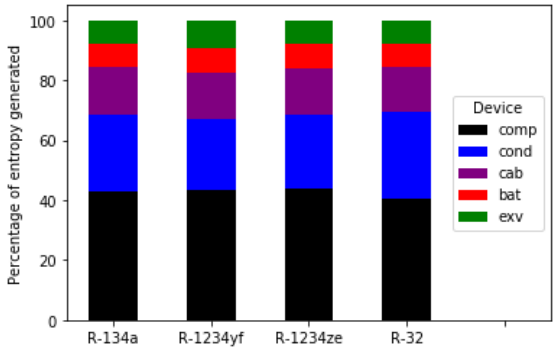

Figure 5: Percentage of entropy generated by each device for the system with evaporators at equal pressure.

destruction of the real cycle is reduced for all devices except for the cabin evaporator, which had no difference in operation. This reduction in exergy destruction is actually the source of improvement in COP for the system. Exergy destruction from the expansion valves had the most significant reduction of all devices, caused by the fact that it is needed less expansion valves to operate the cycle, and the amount of expansion caused by the device is also greatly reduced.

The exergy destruction of the ideal cycle, hence, associated with the refrigerant, has similar characteristics of the previous system, except for the battery evaporator, which is no longer zero. The source of exergy destruction in the battery evaporator is caused by the difference of its temperature and its heat sink, which is no longer zero because the battery evaporator is forced to have the same pressure of the cabin evaporator. Therefore, in the system with evaporators at the same pressure the refrigerant has more influence in the model, yet, the amount of exergy destruction associated with the devices is far greater than the one associated with the refrigerant.

The COP_{ideal} for R-134a, R-1234yf, R-1234ze and R-32 is 35.02, 34.42, 35.17, and 33.81, respectively, which then results to η_{II} of 0.16 for every refrigerant except for R-32, which is 0.15. It is perceived an improvement in second law efficiency, mainly due to the reduction in exergy destruction of the devices of the system. As the refrigerant has greater effect in the exergy destruction of the cycle, its change may results in different values of η_{II}, yet, not significantly. Once again, device improvement, mainly from the compressor, would bring better results than a change in refrigerant.

4. CONCLUSIONS

Regarding the refrigerant fluids, the main conclusions of this work are: R-1234ze had the best performance among the fluids evaluated, followed by R-134a, R-1234yf and R-32; R-32 presented the most distinct results from the average, particularly, operation pressure;

Table 4: Results for the system with evaporators at equal pressure.

	R-134a	**R-1234yf**	**R-1234ze**	**R-32**	**Unit**
COP	5.51	5.38	5.54	5.18	-
$\dot{S}_{gen}$	3.58	3.68	3.56	3.85	W/K
$\dot{m}$	0.0447	0.0563	0.0482	0.0281	kg/s
rot	96.09	99.78	96.40	95.47	Hz
$\dot{W}$	1.27	1.30	1.26	1.35	kW
p_{cond}	11.60	11.54	8.76	27.95	bar
p_{cab}	5.21	5.42	3.88	13.56	bar
p_{bat}	5.21	5.42	3.88	13.56	bar
UA_{cond}	800.3	823.2	815.2	726.6	W/K
UA_{cab}	505.9	507.8	506.3	505.1	W/K
UA_{bat}	155.1	155.5	155.2	154.9	W/K

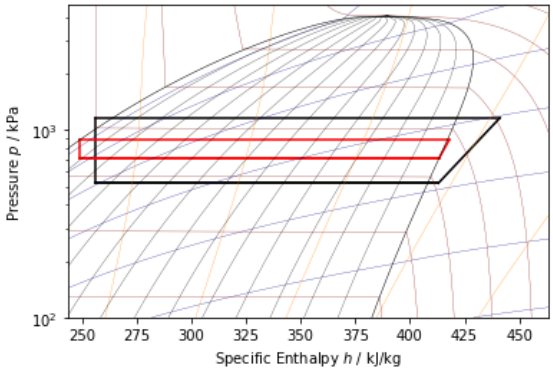

Figure 6: Pressure vs. enthalpy cycle for the system with evaporators at equal pressure for R-134a. Black for real cycle and red for ideal cycle. Cabin and battery evaporator lines overlap.

Table 5: Exergy destroyed by each component for the actual and ideal cycles, for the system with evaporators at the same pressure. Dimension for all values is *W*.

Device	R-134a		R-1234yf		R-1234ze		R-32	
	$\dot{\Psi}_{d,real}$	$\dot{\Psi}_{d,ideal}$	$\dot{\Psi}_{d,real}$	$\dot{\Psi}_{d,ideal}$	$\dot{\Psi}_{d,real}$	$\dot{\Psi}_{d,ideal}$	$\dot{\Psi}_{d,real}$	$\dot{\Psi}_{d,ideal}$
Compressor	474.7	0.00	494.2	0.00	477.9	0.00	479.3	0.00
Condenser	279.0	0.05	268.0	0.00	269.1	0.01	344.8	2.14
Battery evaporator	90.53	20.32	90.36	20.32	90.50	20.32	90.58	20.32
Cabin evaporator	175.5	0.00	175.1	0.00	175.4	0.00	175.6	0.00
Expansion valves	84.28	13.27	106.4	16.80	83.42	12.46	95.03	18.32

The two-stage refrigeration system with evaporators at the same pressure had better performance than the system with evaporators at different pressure.

The main source of irreversibilities in the system is the compressor, followed by the condenser. Expansion valves are a significant source of irreversibilities for the system with evaporators at different pressure. Exergy destruction associated with the devices is far more significant than the exergy destruction associated with the refrigerant. Second law efficiency is about 0.12 and 0.16, for the systems with evaporators at different and same pressure, respectively, regardless of the fluid.

NOMENCLATURE

A	area	(m^2)
COP	coefficient of performance	(-)
h	specific enthalpy	(J/kg)
$\dot{m}$	mass flow rate	(kg/s)
$\dot{Q}$	heat flux	(W)
rot	compressor speed	(Hz)
s	specific entropy	(J/kgK)
U	overall heat transfer coeff.	(W/m^2K)
V	volume	(m^3)
VRE	volumic refrigerant effect	(J/m^3)
$\dot{W}$	power	(W)
η	efficiency	(-)
Ψ	exergy	(J)

Subscript			
bat	battery evaporator	in	inlet/inside
battery	battery	out	outlet/outside
cab	cabin evaporator	real	real cycle
comp	compressor	s	isentropic process
cond	condenser	sh	superheated
d	destruction	sub	subheated
exv	expansion valve(s)	tp	two-phase
G	global	V	volumetric
gen	generated	v	saturated vapor
l	saturated liquid	0	dead state
ideal	idealized cycle	1,2,3,...	states
		II	second law

REFERENCES

Bahman, A. M., & Groll, E. A. (2020). Application of second-law analysis for the environmental control unit at high ambient temperature. *Energies*, *13*(12), 3274.

Bell, I. H., Wronski, J., Quoilin, S., & Lemort, V. (2014). Pure and pseudo-pure fluid thermophysical property evaluation and the open-source thermophysical property library coolprop. *Industrial & Engineering Chemistry Research*, *53*(6), 2498–2508.

Cui, M., Wang, B., Wei, F., & Shi, W. (2022). A modified exergy analysis method for vapor compression systems: Splitting refrigerant exergy destruction. *Applied Thermal Engineering*, *201*(Part A).

Gillet, T., Andrès, E., El-Bakkali, A., Olivier, G., & Lemort, V. (2016). Modelling of an automotive multi-evaporator air-conditioning system. In *Proceedings of the 16th international refrigeration and air conditioning conference.* West Lafayette: Purdue university.

Howe, J. P. (2015). This is nature; this is un-nature: Reading the Keeling curve. *Environmental History*, *20*(2), 286-293.

IEA. (2019). *Global EV outlook 2019.*

Kim, J., Oh, J., & Lee, H. (2019). Review on battery thermal management system for electric vehicles. *Applied Thermal Engineering*, *149*(25), 192-212.

Klein, S. A. (2016). *EES – engineering equation solver.* Version 10.166 (2016-11-20). F-Chart Software.

Krüger, I. L., Limperich, D., & Schmitz, G. (2012). Energy consumption of battery cooling in hybrid electric vehicles. In *Proceedings of the 14th international refrigeration and air conditioning conference.* West Lafayette: Purdue university.

Myhre, G., Shindell, D., Bréon, F.-M., Collins, W., Fuglestvedt, J., Huang, J., … Zhang, H. (2013). Anthropogenic and natural radiative forcing. In *Climate change 2013: The physical science basis. contribution of working group i to the fifth assessment report of the intergovernmental panel on climate change* (p. 659-740). Cambridge and New York: Cambridge University Press.

Peuker, S., & Hrnjak, P. (2006). *Experimental and modeling investigation of two evaporator automotive air conditioning systems.* Urbana-Champaign: Air Conditioning and Refrigeration Center. College of Engineering. University of Illinois.

Shelly, T. J., Weibel, J. A., Ziviani, D., & Groll, E. A. (2021). Comparative analysis of battery electric vehicle thermal management systems under long-range drive cycles. *Applied Thermal Engineering*, *198*.

Stoecker, W. F., & Jones, J. W. (1983). *Refrigeration and air conditioning* (2nd ed.). New York: McGraw-Hill, Inc.

Wang, Q., Jiang, B., Li, B., & Yan, Y. (2016). A critical review of thermal management models and solutions of lithium-ion batteries for the development of pure electric vehicles. *Renewable and Sustainable Energy Reviews*, *64*, 106-128.

ACKNOWLEDGMENT

The authors thank CAPES for the financial support. This research was based upon a R&D Project from ANEEL – PD.0394-1910/2019, supported by Eletrobras Furnas e Serra do Facão Energia, with AVL cooperation.